THERMOELASTIC STRESSES IN PIECEWISE-UNIFORM STRUCTURES

T. G. Beleicheva

UDC 517.949.8:537.319

Many microelectronic devices can be considered as piecewise-uniform structures consisting of materials having different coefficients of thermal expansion and elastic constants. As a result of a difference between operating temperatures and the temperature at which the device was manufactured, large thermal stresses can arise leading to cracking and loss of adhesion in the film–substrate system [1, 2], mechanical rupture of alloy transistors [3, 4], and peeling of semiconductor crystals and the production of cracks in them during the bonding of semiconductor devices to their cases [5-7]. In addition, residual thermal stresses can affect the operating parameters of the devices as a result of the stress dependence of certain physical properties [8-11]. In view of this it becomes necessary to calculate and analyze stresses in such composite media. Existing calculational models for the most part pertain to two-layer systems [10-17]. Stress calculations have been performed in [3, 6, 18, 19] for systems with more than two layers by using hypotheses of thin-beam theory. In actual semiconductor devices, however, the thickness of the structure may be commensurate with the length of the layers; in addition, the layers are generally of different lengths, and experiment shows stress concentrations [20, 21] and the formation of cracks [3, 6, 7] close to the edges. All this in a number of cases makes it impossible to employ calculations [3, 6, 18, 19]. The purpose of the present article is to calculate stresses in piecewise-uniform systems, and from their analysis to estimate the reliability of the functioning of the structures and the choice of appropriate construction and dimensions of the systems, since other requirements (solubility, electrical properties, economy, etc.) may restrict the use of materials which are ideally suited from the point of view of their coefficients of thermal expansion.

1. As a mathematical model applicable to the microelectronics of structures we choose a right circular cylinder D of radius R and height H which is piecewise uniform both axially and radially. Figure 1a shows a section $\theta = \text{const}$ for $0 \leq r \leq R$ (region II) of cylinder D in cylindrical coordinates r, θ, z. The planes S_1 and S_2 parallel to the base of D, and the cylindrical surface S_3 concentric with the lateral surface of D divide D into six cylindrical and ring-shaped regions D_k, each of which is filled with a uniform isotropic elastic medium characterized by a coefficient of thermal expansion α_k, shear modulus G_k, and Poisson's ratio ν_k, where k is the number of the region in Fig. 1a; $k = 1, 2, \ldots, 6$.

The outer boundary S of body D is stress-free, and the conditions of hard contact are satisfied on S_1, S_2, and S_3.

We consider the axisymmetric linear elasticity-theory problem of determining the state of stress of a composite cylindrical body for a variation of its temperature by an amount ΔT. It is assumed that ΔT is uniform in D.

The model shown in Fig. 1a enables us to treat a variety of finite structures of various geometries, some of which are shown schematically in Fig. 1b-*l*. The systems shown in Fig. 1b, c, i (continuous and discontinuous films on a substrate) and in Fig. 1e-h (fastening of crystals in instrument cases) have applications in microelectronics. The same system of coordinates is chosen for the models shown in Fig. 1b-*l* as for the model in Fig. 1a.

In each of the regions D_k the Duhamel–Neumann equilibrium equations [22] in cylindrical coordinates have the form

$$\nabla^2 u - \frac{u}{r^2} + \frac{1}{1-2\nu_k}\frac{\partial e}{\partial r} = 0, \quad \nabla^2 w + \frac{1}{1-2\nu_k}\frac{\partial e}{\partial z} = 0, \tag{1.1}$$

Novosibirsk. Translated from Zhurnal Prikladnoi Mekhaniki i Tekhnicheskoi Fiziki, No. 5, pp. 135-143, September-October, 1979. Original article submitted September 28, 1978.

0021-8944/79/2005-0637 $07.50

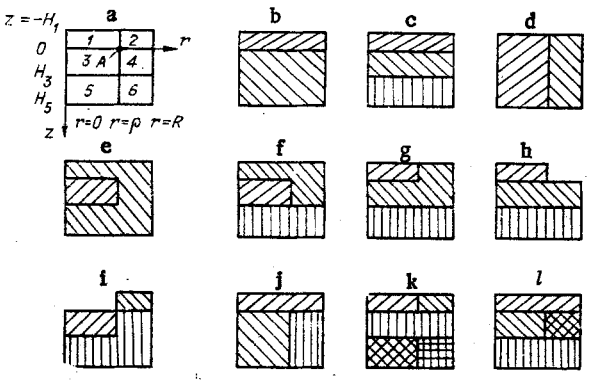

Fig. 1

where

$$e = \frac{\partial u}{\partial r} + \frac{u}{r} + \frac{\partial w}{\partial z}, \quad \nabla^2 = \frac{\partial^2}{\partial r^2} + \frac{1}{r}\frac{\partial}{\partial r} + \frac{\partial^2}{\partial z^2}.$$

Here $u = u(r, z)$ and $w = w(r, z)$ are, respectively, the r and z components of the displacement.

Since there are no external forces on the boundary S we have

$$\begin{aligned} &\sigma_{rr}(R, z) = 0, && \tau_{rz}(R, z) = 0, \\ &\sigma_{zz}(r, -H_1) = 0, && \tau_{rz}(r, -H_1) = 0, \\ &\sigma_{zz}(r, H_5) = 0, && \tau_{rz}(r, H_5) = 0. \end{aligned} \tag{1.2}$$

The stresses and displacements are continuous at the boundary surfaces S_1, S_2, and S_3:

$$\begin{aligned} &\sigma_{zz}(r, +0) = \sigma_{zz}(r, -0), && \tau_{rz}(r, +0) = \tau_{rz}(r, -0), \\ &u(r, +0) = u(r, -0), && w(r, +0) = w(r, -0), \\ &\sigma_{zz}(r, H_3 + 0) = \sigma_{zz}(r, H_3 - 0), && \tau_{rz}(r, H_3 + 0) = \tau_{rz}(r, H_3 - 0), \\ &u(r, H_3 + 0) = u(r, H_3 - 0), && w(r, H_3 + 0) = w(r, H_3 - 0), \\ &\sigma_{rr}(\rho + 0, z) = \sigma_{rr}(\rho - 0, z), && \tau_{rz}(\rho + 0, z) = \tau_{rz}(\rho - 0, z), \\ &u(\rho + 0, z) = u(\rho - 0, z), && w(\rho + 0, z) = w(\rho - 0, z). \end{aligned} \tag{1.3}$$

At $r = 0$ the conditions of axial symmetry are satisfied

$$u(0, z) = 0, \quad \sigma_{rr}(0, z) = \sigma_{\theta\theta}(0, z). \tag{1.4}$$

Here $\sigma_{rr}(r, z)$, $\sigma_{\theta\theta}(r, z)$, and $\sigma_{zz}(r, z)$ are, respectively, the normal radial, tangential, and axial stresses; $\tau_{rz}(r, z)$ is the tangential stress. The parameter ΔT is contained in the differential expressions of Hooke's law for the normal stresses [22]. The parameters α_k, ν_k, G_k, ΔT, R, ρ, and H_k are given. It is required to find the functions $u(r, z)$ and $w(r, z)$ in region II: $0 \le r \le R$, $-H_1 \le z \le H_5$.

2. The linear boundary-value problem (1.1)-(1.4) is reduced to a variational problem for the minimum of the potential energy W of the system. The expression for W for axisymmetric deformation is given in [23]. In region II primary and dual rectangular meshes are superimposed as in [23]. Then W becomes a function of the discrete values $u_{i,j}$ and $w_{i,j}$, where i and j are, respectively, the numbers of the horizontal and vertical lines of the primary mesh $[1 \le i \le p,\ 1 \le j \le q,\ p = 1 + \sum_{k=1,3} (|H_k|/h_z^k + (H_5 - H_3)/h_z^5),\ q = 1 + R/h_r]$.

Here h_r and h_z are the steps of the primary mesh in r and z, respectively (the step h_r is constant; step h_z^k corresponds to region D_k; $h_z^1 = h_z^2$, $h_z^3 = h_z^4$, $h_z^5 = h_z^6$).

The following approximations of derivatives were used:

$$\frac{1}{r}\frac{\partial}{\partial r}(ru) \approx \frac{u_{i,j+1} - u_{i,j}}{h_r} + \frac{u_{i,j}}{r_j},$$

$$\frac{\partial u}{\partial r} \approx \frac{u_{i,j+1} - u_{i,j}}{h_r}, \quad \frac{\partial u}{\partial z} \approx \frac{u_{i,j} - u_{i+1,j}}{h_z^k},$$

$$\frac{\partial w}{\partial r} \approx \frac{w_{i,j+1} - w_{i,j}}{h_r}, \quad \frac{\partial w}{\partial z} \approx \frac{w_{i,j} - w_{i+1,j}}{h_z^k}.$$

The approximate expression for W_{ij}^l for an interior cell of region II (a cell formed by lines of the primary and dual meshes) has the form

$$W_{i,j}^l = \sum_{n=1}^{5} a_{j,n,k} \left[L_n^l(u_{i,j}) + P_n^l(w_{i,j})\right]^2$$
$$+ b_{j,k} \left[L_1^l(u_{i,j}) + P_1^l(w_{i,j})\right] + c_{j,k}, \quad k = 1, 2, \ldots, 6,$$

where L_n and P_n are certain linear difference operators, and $a_{j,n,k}$, $b_{j,k}$, and $c_{j,k}$ are constant within each cell. The superscript l refers to one of the four cells surrounding the interior point (i, j).

The expression for W was obtained by summing expressions of the form (2.1) over i, j, and l (for points $(i, j) \in S$ the superscript $l = 1, 2$).

Difference equations approximating the original differential equations (1.1)-(1.4) with an accuracy of the order $O(h^2)$, $h = \max(h_r, h_z^k)$, were obtained from the stationarity conditions

$$\partial W/\partial u_{i,j} = 0; \tag{2.2}$$
$$\partial W/\partial w_{i,j} = 0. \tag{2.3}$$

In particular, condition (2.2) for point A (cf. Fig. 1a) has the form

$$(2.4)\Bigg\{2\left[\frac{1}{(j-1)h_r} + \frac{2j}{h_r}\right]\sum_{k=1}^{4}\psi_k h_z^k + \frac{(j-1)h_r^2}{2}\sum_{k=1}^{4}\frac{G_k}{h_z^k} - \frac{2}{h_r}\left[\sum_{k=2,4}\lambda_k(1+\nu_k)h_z^k$$
$$+ \sum_{k=1,3}\lambda_k(3-5\nu_k)h_z^k\right]\Bigg\}u_{i,j} - \frac{(j-1)h_r^2}{2}\sum_{k=1,2}\frac{G_k}{h_z^k}u_{i+1,j} - \frac{(j-1)h_r^2}{2}\sum_{k=3,4}\frac{G_k}{h_z^k}u_{i-1,j}$$
$$- \frac{2(2j-1)}{h_r}\sum_{k=2,4}\psi_k h_z^k u_{i,j+1} - \frac{2(2j-3)}{h_r}\sum_{k=1,3}\psi_k h_z^k u_{i,j-1}$$
$$- \left[(j-1)\left(\sum_{k=2,3}\lambda_k - \sum_{k=1,4}\lambda_k\right) + 2\left(\sum_{k=3,4}\chi_k - \sum_{k=1,2}\chi_k\right)\right]w_{i,j}$$
$$+ \{\lambda_2[(1-6\nu_2) - j(1-4\nu_2)] - \lambda_1[(1-2\nu_1) - j(1-4\nu_1)]\}w_{i+1,j}$$
$$- \{\lambda_4[(1-6\nu_4) - j(1-4\nu_4)] - \lambda_3[(1-2\nu_3) - j(1-4\nu_3)]\}w_{i-1,j}$$
$$+ [(j-1)(G_2 - G_4) - 2j(\chi_2 - \chi_4)]w_{i,j+1} - [(j-1)(G_1 - G_3)$$
$$-2(j-2)(\chi_1 - \chi_3)]w_{i,j-1} + [(j-1)\lambda_2 + 2\chi_2]w_{i+1,j+1} - [(j-1)\lambda_4 + 2\chi_4]$$
$$\times w_{i-1,j+1} - [(j-1)\lambda_1 - 2\chi_1]w_{i+1,j-1} + [(j-1)\lambda_3 - 2\chi_3]w_{i-1,j-1}$$
$$= 4(j-1)\Delta T\left[\sum_{k=1,3}\lambda_k(1+\nu_k)\alpha_k h_z^k - \sum_{k=2,4}\lambda_k(1+\nu_k)\alpha_k h_z^k\right], \tag{2.4}$$

where

$$\lambda_k = \frac{G_k}{1-2\nu_k}\frac{h_r}{4}; \quad \chi_k = \lambda_k\nu_k; \quad \psi_k = \lambda_k(1-\nu_k).$$

By making appropriate replacements of the constants in (2.4) the equations $\partial W/\partial u_{i,j} = 0$ are obtained for boundaries S_1, S_2, and S_3, and for interior points of region D_k (e.g., for region D_1 it is necessary to set $\alpha_k = \alpha_1$, $G_k = G_1$, $\nu_k = \nu_1$, $h_z^k = h_z^1$, $k = 1, 2, 3, 4$).

A nine-point difference scheme is obtained. All the unknowns are grouped in vertical lines in column vector form

$$\eta_j = \begin{Vmatrix} u_{1,j} \\ w_{1,j} \\ u_{2,j} \\ w_{2,j} \\ \vdots \\ u_{p,j} \\ w_{p,j} \end{Vmatrix}.$$

A system of $2 \times p \times q$ linear inhomogeneous algebraic equations in the same number of unknowns $u_{i,j}$ and $w_{i,j}$ is formed by varying the subscripts in Eqs. (2.2) and (2.3), starting with $j = 1$ for $i = 1, 2, \ldots, p$ etc. in order of increasing j for the same values of i, so that to each $u_{i,j}$ there correspond $[2p(j-1) + 2i - 1]$ equations, and to each $w_{i,j}$ $[2p(j-1) + 2i]$ equations.

This order of arranging the unknowns and equations produces a block tridiagonal form of matrix A of the coefficients of the unknowns $u_{i,j}$ and $w_{i,j}$. This makes it possible to solve the system of equation numerically by the successive line overrelaxation method [24]. The solutions for the diagonal blocks of matrix A are found by the Gauss single-division scheme [25]. The condition for ending the iterative process has the form

$$\delta = \max_{i,j} \left| \eta_j^{(m+1)}(i) - \eta_j^{(m)}(i) \right| < \varepsilon, \quad m = 1, 2, \ldots,$$

where ε is the accuracy of the iterations.

The error of the solution was estimated by calculating the quantity

$$\varphi = \max_{i,j} (\varphi_{i,j}, \psi_{i,j}), \quad \varphi_{i,j} = \left| u_{i,j}^h - u_{i,j}^{2h} \right| / \left| u_{i,j}^h \right|,$$
$$\psi_{i,j} = \left| w_{i,j}^h - w_{i,j}^{2h} \right| / \left| w_{i,j}^h \right|,$$

where $u_{i,j}^h$, $w_{i,j}^h$ and $u_{i,j}^{2h}$, $w_{i,j}^{2h}$ are the solutions obtained for meshes with steps h_r, h_z^k, and $2h_r$, $2h_z^k$, respectively.

3. The algorithm described above was programmed for the model shown in Fig. 1a. By starting from one program it was possible to calculate a variety of final systems of various geometries, in particular the systems shown in Fig. 1b-h, k, *l*. The calculations were performed on a BÉSM-6 computer; the optimum relaxation parameter [24] $\omega_{opt} = 1.9$ was chosen by numerical experiments. The initial iteration vector $\eta_j^{(0)}$ was chosen with zero components for all j.

The program was first tested on a number of models of cylinders: "unheated," uniform, symmetric with respect to the center of mass. For $\Delta T = 0$ ("unheated" cylinder) the calculation gave zero solutions for all $u_{i,j}$, $w_{i,j}$, σ_{rr}, $\sigma_{\theta\theta}$, σ_{zz}, and τ_{rz}. In the calculation of uniform cylinders ($\alpha_k = \alpha$, $\nu_k = \nu$, $G_k = G$, $k = 1, 2, \ldots, 6$) displacements were obtained corresponding to free contraction and zero stresses with a maximum error of ~ 0.02 kg/mm^2. In cylinders which were symmetric with respect to the center of mass (Fig. 1c-e, k, *l*) agreement to eight significant figures was found in the values of the stresses along lines i equidistant from the center of mass of D.

Figure 2 shows curves of the distribution of errors $\varphi_{i,j}$ (solid curves) and $\psi_{i,j}$ (open curves) along the radius for the system shown in Fig. 1g (region D_1 – silicon; D_2, D_3, D_4 – lead borate glass; D_5, D_6 – Polycore). Points 1 and 2 refer, respectively, to sections $z = 0$ and $z = 0.004$. The system was cooled by $\Delta T = 470$°C and had the following dimensions (here and later in cm): $R = 0.3$, $H_1 = 0.024$; $H_3 = 0.006$; $H_5 - H_3 = 0.175$. The solutions obtained on two meshes with the total number of points 110 and 399 were compared. In spite of the fact that one of the meshes was rather coarse, the value of φ did not exceed 3%.

Our results were compared with solutions existing in the literature. In the absence of radial boundaries, and for $2R/H \gg 1$ we have the structure of [18] (Fig. 1c). Table 1 compares our results with those of [18] for a Si–Au–Kovar system cooled by $\Delta T = 400$°C and having the following dimensions: $R = 0.1$, $H_1 = 0.03$,

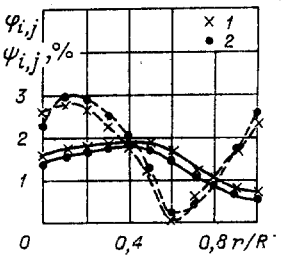

Fig. 2

TABLE 1

r/R	0	0,1	0,2	0,3	0,4	0,5	0,6	0,7	0,8	0,9	[18]
$\varepsilon=0{,}0006$	54,59	54,56	54,64	54,66	54,69	54,67	54,67	54,64	54,53	53,89	54,13
$\varepsilon=-0{,}006$	—4,43	—4,42	—4,38	—4,36	—4,35	—4,31	—4,25	—4,12	—3,83	—3,04	—4,01
$\varepsilon=-0{,}024$	1,002	1,00	0,99	0,94	0,89	0,85	0,79	0,70	0,53	0,25	1,08
$\varepsilon=0{,}0096$	—1,31	—1,31	—1,14	—1,08	—1,05	—1,05	—1,09	—1,18	—1,25	—1,00	—1,02

TABLE 2

r	0,0125	0,025	0,0375	0,05	0,0625	0,075	0,0875	0,1125	0,1250	0,1375	0,150	0,1625	0,175	0,1875
σ_{rr}	—1,735	—1,738	—1,732	—1,757	—1,839	—1,984	—1,875	—1,415	—0,8235	—0,6015	—0,443	—0,3012	—0,1800	—0,0816
σ_{rr}^*	—1,764	—1,764	—1,764	—1,764	—1,764	—1,764	—1,764	—1,270	—0,917	—0,656	—0,457	—0,3028	—0,1799	—0,0811
$\sigma_{\theta\theta}$	—1,735	—1,738	—1,731	—1,735	—1,748	—1,797	—1,929	2,496	2,087	1,800	1,605	1,453	1,333	1,236
$\sigma_{\theta\theta}^*$	—1,764	—1,764	—1,764	—1,764	—1,764	—1,764	—1,764	2,406	2,093	1,832	1,633	1,478	1,356	1,257

TABLE 3

	$\alpha\cdot10^5$, 1/deg	$G\cdot10^{-6}$, kg/cm^2	ν	R	ρ	H_1	H_3	H_5-H_3	ΔT
Si	0,42	0,664	0,28						
Lead borate glass	0,75	0,27	0,2	0,3	0,18	0,024	0,006	0,175	470°C
Polycore	0,75	1,2	0,45						

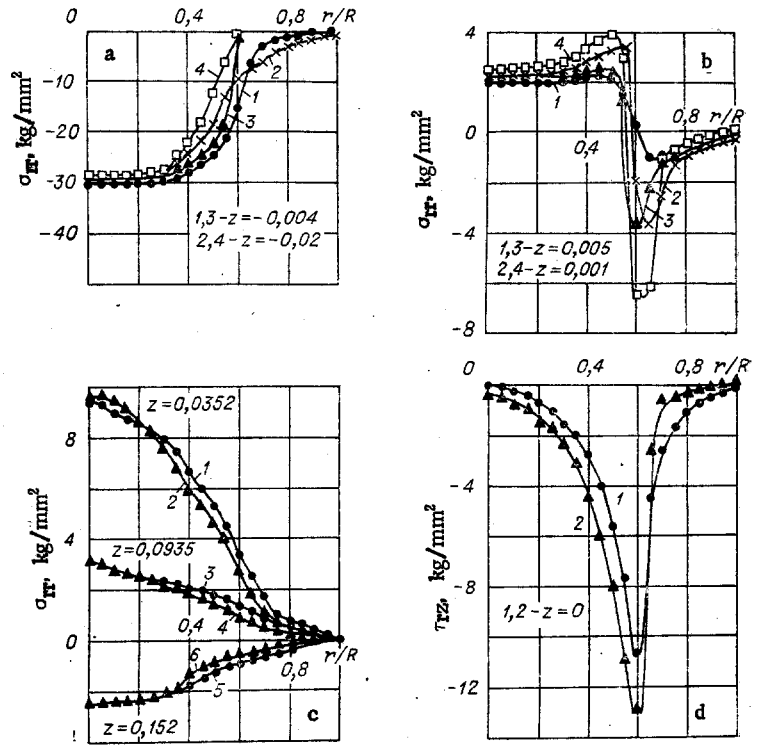

Fig. 3

$H_3 = 0.001$, $H_5 - H_3 = 0.012$. In the calculation with the model in [18] $E_k/(1 - \nu_k)$ was used instead of E_k, where E_k is Young's modulus. In the absence of axial boundaries and for $2R/H \gg 1$ we obtain the radially composite disk shown in Fig. 1d whose solution is given in [26]. Table 2 compares our values of the stresses σ_{rr} and $\sigma_{\theta\theta}$ in kg/mm^2 at points along the radius of the central z cross section with those calculated from the equations of [26] for an Si-Mark K-81-39 plastic system (the inner solid cylinder is Si). The system was cooled by $\Delta T = 130°C$ and had the following dimensions: $R = 0.2$, $\rho = 0.1$, $H = 0.03$. Tables 1 and 2 show that our results are in good agreement with those of [18, 26].

It should be noted that in contrast with [18, 26] our procedure makes it possible to treat systems with $2R/H \approx 1$, and to obtain coordinate distributions of both tangential and all the components of the normal stresses, while only the z distribution of σ_{rr} can be calculated by the method in [18], and only the r distribution of σ_{rr} and $\sigma_{\theta\theta}$ by [26].

As an example Fig. 3 shows the calculated values of the stresses for the nonuniform structures shown in Fig. 1g (system A) and Fig. 1h (system B). Systems A and B correspond to the two limiting cases of fastening an Si crystal (region D_1) to a Polycore case (regions D_5 and D_6) of the integral scheme: in A the crystal is completely embedded in lead borate glass (regions D_2, D_3, and D_4) to the level of its upper surface; in B the crystal is in contact with glass (regions D_3 and D_4) on only one surface. Table 3 lists the values of the material constants used, ΔT, and the dimensions of the systems.

Figures 3a-c show, respectively, the radial distributions of the normal stress σ_{rr} for $-H_1 < z < 0$, $0 < z < H_3$, and $H_3 < z < H_5$. Figure 3d shows the dependence of the tangential stress τ_{rz} on r/R. In the layer $z < 0$ the silicon and glass are under compression (Fig. 3a). The state of stress in Si up to $r/R \sim 0.3$ is planar and practically the same in system A (curves 1, 2) as in B (curves 3, 4). The normal tensile stress in the glass layer ($0 \leq z \leq 60$ μm) becomes compressive for $r/R \sim \rho$ (Fig. 3b). The level of dangerous tensile stresses in the glass layer in system B (curves 3, 4) is somewhat higher than in A (curves 1, 2). In Polycore (Fig. 3c) there are no significant differences between system A (curves 1, 3, 5) and system B (curves 2, 4, 6). The layers of Polycore adjoining glass (curves 1, 2) are under tension, but close to the free boundary (curves 5, 6) under compression. The shear stresses (Fig. 3d) in systems A (curve 1) and B (curve 2) are comparable in magnitude with the normal stresses and are concentrated about the point $r = \rho$, $z = 0$. The most dangerously stressed region is in glass adjacent to the point $r = \rho$, $z = 0$. The large value of τ_{rz} indicates the possibility of the separation of the silicon crystal from the glass. Figure 3 shows that embedding the crystal in glass (system A) is preferable to attaching it to the surface (system B). The stress

in Si resulting from setting crystals in the case is two orders of magnitude above that produced in Si in obtaining a continuous layer of SiO_2 [15, 17]. It should be noted that it is impossible to determine the stress–strain state in the vicinity of nodal points with complete reliability if the edge effect is damped out (Fig. 3b) within the limits of one step of the mesh.

The author thanks K. K. Ziling for helpful comments during a discussion of the work.

LITERATURE CITED

1. R. Zeyfang, "Stresses in epitaxially grown single-crystal films: YIG on YAG," J. Appl. Phys., 41, No. 9 (1970).
2. D. S. Campbell, Handbook of Thin Film Technology, L. I. Maissel and R. Gland (editors), McGraw-Hill, New York (1970).
3. T. C. Taylor, "Thermally induced cracking in the fabrication of semiconductor devices," IRE Trans. Electron Devices, 6, No. 3 (1959).
4. D. A. Jenny, "A germanium n–p–n alloy junction transistor," Proc. IRE, 41, No. 12 (1953).
5. R. Zeyfang, "Residual stresses in thin single crystals bonded to an amorphous substrate: silicon-integrated circuits," J. Appl. Phys., 42, No. 3 (1971).
6. T. C. Taylor and F. L. Yuan, "Thermal stresses and fracture in shear-constrained semiconductor device structures," IRE Trans. Electron Devices, ED-9, No. 3 (1962).
7. T. D. Riney, "Residual thermoelastic stresses in bonded silicon wafers," J. Appl. Phys., 32, No. 3 (1961).
8. H. F. Matare, Defect Electronics in Semiconductors, Wiley-Interscience, New York (1971).
9. G. Abowitz, E. Arnold, and J. Ladell, "Symmetry of interface charge distribution in thermally oxidized silicon," Phys. Rev. Lett., 18, No. 14 (1967).
10. J. H. Serebrinsky, "Stress concentration in silicon–insulator interfaces," Solid-State Electron., 13, No. 11 (1970).
11. T. Sugano and K. Kakemoto, "Mechanical stresses and strains in Si–SiO_2 interface and its influence on transistor characteristics," in: Mikroelektronik 2, Vorträge der 2 Mikroelektronik-Tagung des "Internationalen Elektronik-Arbeitskreises eV" (INEA) in München, October, 1966, 24-26, R. Oldenbourg, Munich and Vienna.
12. S. P. Timoshenko, Stability of Rods, Plates, and Shells [in Russian], Nauka, Moscow (1971).
13. B. J. Aleck, "Thermal stresses in a rectangular plate fastened along its edge," J. Appl. Mech., 16, No. 2 (1949).
14. R. Zeyfang, "Stresses and strains in a plate fastened on a substrate: semiconductor devices," Solid-State Electron., 14, No. 10 (1971).
15. S. D. Brotherton, T. G. Read, D. R. Lamb, and A. F. Willoughby, "Surface charge and stress in the Si–SiO_2 system," Solid-State Electron., 16, No. 12 (1973).
16. G. F. Pishchik, E. N. Prokof'ev, O. E. Ol'khovik, and L. V. Sergeev, "Thermal stresses in two-layer isotropic optical plates," Opt.-Mekh. Promyshlennost', No. 10 (1964).
17. T. G. Beleicheva and K. K. Ziling, "A thermoelastic asixymmetric problem for a two-layer cylinder," Prikl. Mekh. Tekh. Fiz., No. 1 (1978).
18. É. I. Grigolyuk and V. M. Tolkachev, "Theory of a multilayer thermostat," Izv. Sib. Otd. Akad. Nauk SSSR, Ser. Tekh. Nauk, 10, No. 3 (1963).
19. H. J. Oel and V. D. Frechette, "Stress distribution in multiphase systems: 1. Composites with planar interfaces," J. Am. Ceram. Soc., 50, No. 10 (1967).
20. I. A. Blech and E. S. Meieran, "Enhanced x-ray diffraction from substrate crystals containing discontinuous surface films," J. Appl. Phys., 38, No. 7 (1967).
21. B. C. Wonsiewicz and D. V. McCaughan, "Electrical properties of metal–SiO_2–silicon structures under mechanical stress," J. Appl. Phys., 44, No. 12 (1973).
22. B. A. Boley and J. H. Weiner, Theory of Thermal Stresses, Wiley, New York (1960).
23. D. S. Griffin and R. B. Kellog, "A numerical solution for axially symmetrical and plane elasticity problems," Int. J. Solids Struct. 3, No. 5 (1967).
24. G. E. Forsythe and W. R. Wasow, Finite Difference Methods for Partial Differential Equations, Wiley, New York.
25. D. K. Faddeev and V. N. Faddeeva, Computational Methods of Linear Algebra [in Russian], Fizmatgiz, Moscow (1960).
26. S. S. Gurin and E. N. Lambina, "Approximate calculation of thermoelastic stresses in bimetallic castings," in: Theoretical and Applied Mechanics [in Russian], No. 2, Vyshéish. Shkola (1975).